

EXPERIMENTAL STUDY OF ELECTROOSMOTIC FLOW IN THIN SLIT CHANNELS

V. V. Kadet and P. S. Koryuzlov

UDC 532.546

This paper gives the results of experimental studies of flow of two immiscible liquids in a thin slit channel under the action of an external electric field. A comparison is made of numerical calculation results and experimental data on the time dependence of the position of the interface. The employed model is shown to provide an adequate qualitative description of electroosmotic flow in thin slit channels of width not less than 20 μm .

Key words: electroosmotic flow, electric double layer, thin slit channels.

Use of electrical technologies in various branches of the mining industry (underground leaching of metals, oil extraction, and water supply) requires a detailed study of liquid electrolyte flow in porous media. It should be taken into account that, as the channel pore size decreases to the scale of micropores (of the order of 10 μm), interfacial interaction begins to have a significant effect on the liquid flow. The results of experimental studies of microchannel flow suggest that the electric double layer has a significant effect on the velocity field distribution and the effective liquid viscosity. Electroosmotic flow in microchannels has been studied in a series of experiments using high-speed photography [2]. Similar studies providing visualization of electroosmotic flow in microchannels have been performed for the case of intersection of channels [3] and for the case of a cylindrical channel with a uniformly distributed surface charge in the electric double layer [4]. Experimental studies [5] have shown that, for flow of dilute electrolytes in rectangular microchannels the hydraulic resistance coefficients are abnormally high compared to the values obtained for channels of large radius, in which electrokinetic effects are negligibly small. These data served as the basis for theoretical modeling of single-phase electroosmotic flow in a porous medium [6]. Models of two-phase electroosmotic flow have been proposed [7–9]. However, until recently, no experimental studies have been performed in this area, in particular, for the case of flow in a thin slit channel.

The present paper gives the results of experiments in which the position of the interface between two immiscible liquids flowing in a thin slit channel was determined and compared with the results of calculations using the model of [1] extended to the case of two-phase flow.

We consider a slit channel of length L and width H filled with liquids having different electrokinetic properties (Fig. 1).

Using the results of [1], we calculate the time dependence of the velocity of motion of the interface with two-phase displacement of the liquid in a thin slit channel under the action of an external electric field. In this case, the equation of motion can be written as

$$\frac{d^2U_i}{dy^2} = \frac{1}{\mu_i} \left(\frac{dp}{dx} - \rho_i F_{xi}(y) \right), \quad (1)$$

where the subscript $i \equiv r, l$ corresponds to the liquid on the right and left of the meniscus, respectively. The flow is assumed to be continuous, and the liquid incompressible.

Gubkin Russian State University of Oil and Gas, Moscow 117485: korjuzlov.pavel@gmail.com. Translated from *Prikladnaya Mekhanika i Tekhnicheskaya Fizika*, Vol. 50, No. 5, pp. 90–94, September–October, 2009. Original article submitted November 28, 2007; revision submitted August 1, 2008.

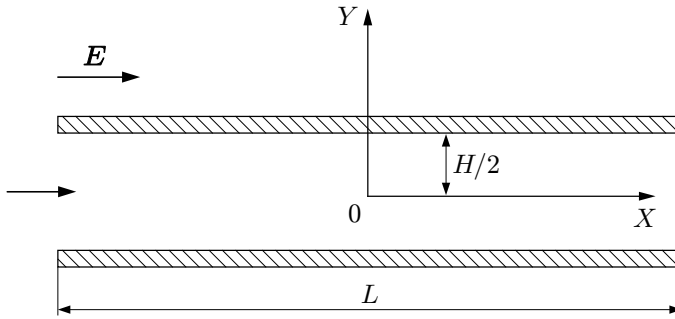


Fig. 1. Diagram of the slit channel: the arrows show the direction of the flow and the direction of the electric-field strength vector.

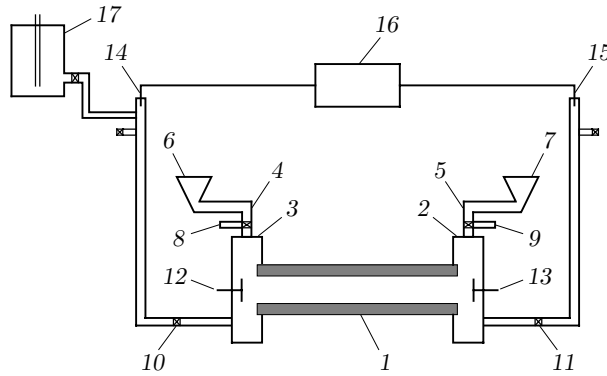


Fig. 2. Diagram of the setup for studies of electroosmotic flow in thin slits: slit channel (1), edges of the slit channel (2 and 3), leads (4 and 5), measuring channels (6 and 7), valves (8–11), electrodes (12–15), constant-voltage source (16), and Prandtl vessel (17).

The interaction of each liquid with the surface is characterized by a zeta potential whose distribution can be calculated using the equation

$$\frac{d^2\Psi}{d\bar{y}^2} = \sinh \Psi(\bar{y}),$$

where $\bar{y} = \kappa y$ ($1/\kappa$ is the thickness of the diffuse part of the electric double layer or the Debye–Hückel parameter).

We integrate Eq. (1) twice over the entire thickness of the channel opening and equate the obtained expressions for the velocities on the right and left of the interface using the flow continuity conditions. As a result, we obtain

$$x_f = \frac{x_f(A - B) + BL}{\mu_r L + x_f(\mu_l - \mu_r)}, \quad (2)$$

where

$$A = 4 \int_0^{H/2} \int_0^{H/2} \rho_l F_{x,l}(y) dy dy; \quad B = 4 \int_0^{H/2} \int_0^{H/2} \rho_r F_{x,r}(y) dy dy;$$

x_f is the position of the interface, μ_l and μ_r are the viscosities of the liquids on the left and right of the interface, respectively, ρ_l and ρ_r are the densities of the liquids, and $F_{x,l}(y)$ and $F_{x,r}(y)$ are the body forces acting on the space charges which can be determined from the Poisson–Boltzmann equation [10].

To verify the results of calculations using relation (2), we performed a series of experiments to determine the time dependence of the position of the interface. A diagram of the experimental setup is given in Fig. 2. A slit channel 1 consisting of glass plates imposed [3] on each other in a certain manner is placed between the edges of a portable hydrodynamic tunnel. To prevent liquid leakage at the junctions, the edges 2 and 3 of the slit channel are clamped with a rubber clip fixed by tightening bolts located on the perimeter of these edges. Measuring

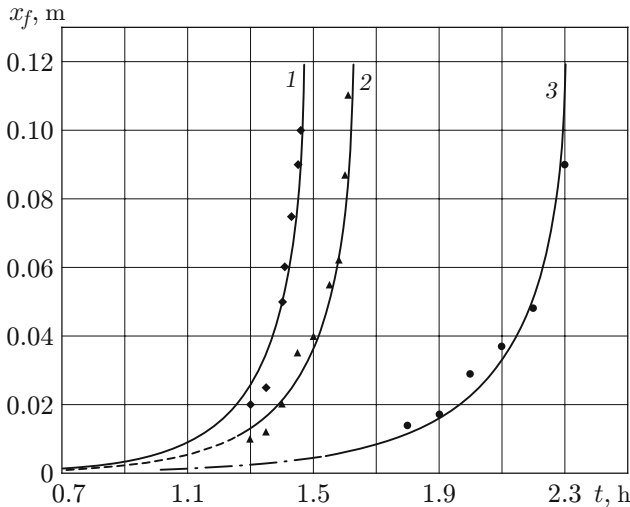


Fig. 3

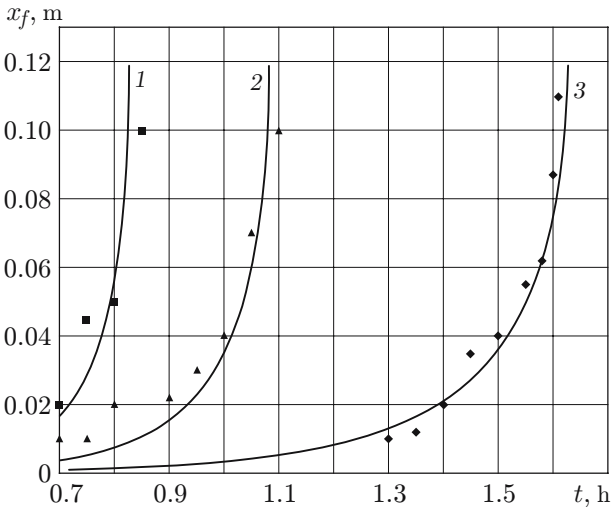


Fig. 4

Fig. 3. Curve of $x_f(t)$ for electric-field strengths $E = 83$ (1), 75 (2), and 53 V/cm (3): curves correspond to calculations and points to experiment; $H = 50 \mu\text{m}$ and $\Psi = 97$ mV.

Fig. 4. Dependence $x_f(t)$ for zeta potential $\Psi = 110$ (1), 93 (2), and 87 mV (3): curves correspond to calculations and points to experiment; $E = 75$ V/cm and $H = 50 \mu\text{m}$.

channels 6 and 7 are connected to the hydrodynamic tunnel by leads 4 and 5 to record the liquid volume flow rate in electroosmotic flow. Valves 8–11 serve to fill the setup with the filtering liquid and evacuate it. Electrodes 12 and 13 are used to apply voltage or measure the potential difference if voltage is applied through electrodes 14 and 15. The constant-voltage source 16 creates an electric potential difference necessary for electroosmotic flow generation. The Prandtl vessel 17 is used to wash and fill the slit channel with an appropriate solution.

The transparent wall of the slit channel allows direct observations and measurements of the interface between the displacing and displaced liquids during their simultaneous flow.

In the experiment, we used aqueous solutions of NaCl with concentrations 0.010, 0.005, and 0.001 mole/liter corresponding to moderate and large values of the zeta potential. Preliminarily, in a channel of greater width ($H = 100 \mu\text{m}$), zeta potentials were determined for the material of the slit-channel walls. The displaced liquid was mineral oil with viscosity $14 \cdot 10^{-3} \text{ Pa} \cdot \text{sec}$ at a temperature of 20°C . After that, the position of the interface x_f was determined for various times and various values of the field strength, zeta potentials of the displacing solutions, and channel width. The coordinate of the interface x_f was calculated by averaging its minimum and maximum values at a given time.

Figure 3 shows the position of the interface versus time for various values of the field strength.

Figure 4 gives the position of the interface versus time for various values of the zeta potential of the displacing solution (field strength $E = 75$ V/cm, channel width $H = 50 \mu\text{m}$).

We note that the smoothness of the interface is significantly deteriorated with increasing zeta potential.

For a channel of width $H = 10 \mu\text{m}$ and a zeta potential $\Psi = 97$ mV, the calculated velocity of the interface is almost 1.5 times lower than the experimentally observed value. This can be explained by the fact that, in a channel of small width, the effect of its surface conductivity increases considerably. Because our model ignores this phenomenon, a possible method for modifying the model is preliminary determination of the effective zeta potential for such a channel width. For a large channel width ($H = 100 \mu\text{m}$), the difference between the calculated velocity and the measured value is 9%.

Conclusions. The results of the experiments show that, at a slit channel width $H > 20 \mu\text{m}$, the model [1] extended to the case of two-phase flow adequately describes the displacement in thin slit channels with two-phase electroosmotic liquid flow for moderate and large values of the zeta potential.

The proposed method allows a sufficiently accurate analysis of the effect of the external electric-field strength and concentration of the displacing electrolyte solution (zeta potential) on the time dependence of the velocity of the displacement front for two-phase flow in a thin slit. However, for a channel width $H \leq 20 \mu\text{m}$, the calculation error increases to 50%, necessitating a correction for the surface conductivity of the channel. This correction can be obtained by additionally measuring the effective zeta potential for this channel width.

REFERENCES

1. N. A. Patankar and H. H. Hu, "Numerical simulation of electroosmotic flow," *Anal. Chem.*, **70**, 1870–1881 (1998).
2. M. G. Garguilo, J. I. Molho, J. G. Santiago, et al., "Electroosmotic capillary flow with nonuniform zeta potential," *Anal. Chem.*, **72**, 1053–1057 (2000).
3. E. B. Cummings, S. K. Griffiths, and R. H. Nilson, "Irrotationality of uniform electroosmosis," in: *Microfluidic Devices and Systems*, Proc. of the 2nd SPIE Conf. (Santa Clara, September 20, 1999), SPIE, Santa Clara (1999), pp. 180–189.
4. J. M. Molho, A. E. Herr, M. Desphande, et al., "Fluid transport mechanisms in micro fluidic devices," in: *Proc. of the ASME Int. Mech. Eng. Congress and Exposition* (Anaheim, November 15–20, 1998), ASME Books, New York (1998), pp. 69–76.
5. F. Bianchi and R. Ferrigno, "Finite element simulation of an electroosmotic-driven flow division at a T-junction of microscale dimensions," *Anal. Chem.*, **72**, 1987–1993 (2000).
6. Y. Kang, Ch. Yang, and X. J. Huang, "Electroosmotic flow in fine grained porous media," *J. Micromech. Microeng.*, No. 14, 1249–1257 (2004).
7. S. Jacky, H. Lee, and Dongqing Li, "Electroosmotic flow at a liquid–air interface," *Microfluidics Nanofluidics*, **2**, No. 4, 361–365 (2006).
8. Shulin Zeng, Chuan-Hua Chen, Juan G. Santiago, et al., "Fréchet electroosmotic flow pumps with polymer frits," *Sensors Actuators, B: Chem.*, **82**, Nos. 2/3, 209–212 (2002).
9. A. Brask, G. Goranović, M. J. Jensen, and H. Bruus, "A novel electro-osmotic pump design for nonconducting liquids: theoretical analysis of flow rate-pressure characteristics and stability," *J. Micromech. Microeng.*, No. 15, 883–891 (2005).
10. Yu. G. Frolov, *Course in Colloidal Chemistry (Surface Phenomena and Disperse Systems)*: College Textbook [in Russian], Khimiya, Moscow (1982).